DOI: 10.37990/medr.1102477
Med Records 2022;4(3):355-60

MEDICAL RECORDS-International Medical Journal

Research Article

The Precise Location of the Stylomastoid Foramen and Clinical Implication for Facial Nerve Block

Foramen Stylomastoideum'un Kesin Konumu ve Fasiyal Sinir Bloğu için Klinik Önemi

Serdar Babacan[1], Rohat Bayat[2], Evren Buyukfırat[3], Mustafa Deniz[1]

[1]Harran University, Faculty of Medicine, Department of Anatomy, Sanlıurfa Turkey
[2]Harran University, Faculty of Medicine, 2nd Year Medical Student, Sanlıurfa, Turkey
[3]Harran University, Faculty of Medicine, Department of Anesthesia and Reanimation, Sanlıurfa, Turkey

Abstract

Aim: We aimed to develop linear regression formulas for determining the precise localization of the stylomastoid foramen on the base of the morphometric features of the person's own skull.

Material and Method: The study was conducted on 22 stylomastoid foramina (11 skulls). The 10 parameters determined for the stylomastoid foramen were measured on the photographs taken from the skull base and the 17 parameters determined for the morphometric features of the skull were measured on the photographs taken from the anterior plane, lateral plane, and posterior plan using Image J measurement software. The data obtained were evaluated with SPSS 20.0 statistical software.

Results: To determine the morphometric and topographic features of the stylomastoid foramen the equations have been developed such as; P1 (The distance between stylomastoid foramen and root of the zygomatic arch)=18.758+(0.472xP12)-(2.092xP16)+(0.831xP17)–(0.390xP18)–(0.101x P20); Adjusted R^2=0.865, Standard Error of the Estimation=1.389.

Conclusion: Mean values can give misleading information in determining the topographical relationship between the stylomastoid foramen and the surrounding anatomical structures. We have developed regression formulas that will estimate the accurate location of the stylomastoid foramen and the accurate distances between other surrounding anatomical structures, taking into account the morphometric characteristics of the person's own skull.

Keywords: Stylomastoid foramen, facial nerve, facial nerve block

Öz

Amaç: Çalışmanın amacı, kişinin kendi kafatasının morfometrik özelliklerinden yola çıkarak foramen stylomastoideum'un kesin lokalizasyonunu belirlemek için lineer regresyon formülleri geliştirmektir.

Materyal ve Metot: Çalışma, 22 foramen stylomastoideum (11 kafatası) üzerinde gerçekleştirildi. Foramen stylomastoideum için belirlenen 10 parametre kafa tabanından çekilen fotoğraflarda, kafatasının morfometrik özellikleri için belirlenen 17 parametre ise Image J ölçümü kullanılarak ön, yan ve arka plandan çekilen fotoğraflarda ölçüldü. Ölçümlerden elde edilen veriler istatistik yazılımı SPSS 20.0 ile değerlendirildi.

Bulgular: Foramen stylomastoideum'un morfometrik ve topografik özelliklerini belirlemek için; P1 (Foramen stylomastoideum ile arcus zygomaticus kökü arası mesafe)=18,758+(0,472xP12)-(2,092xP16)+(0,831xP17)–(0,390xP18)–(0,101xP20); Düzeltilmiş R^2=0.865, Tahminin Standart Hatası=1.389 şeklinde denklemler geliştirilmiştir.

Sonuç: Ortalama değerler, foramen stylomastoideum ve onu çevreleyen anatomik yapılar arasındaki topografik ilişkinin belirlenmesinde yanıltıcı bilgi verebilir. Kişinin kendi kafatasının morfometrik özelliklerini dikkate alarak, foramen stylomastoideum'un kesin konumunu ve çevredeki diğer anatomik yapılar arasındaki doğru mesafeleri belirleyecek regresyon formülleri geliştirdik.

Anahtar Kelimeler: Foramen stylomastoideum, nervus facialis, fasiyal sinir bloğu

INTRODUCTION

The stylomastoid foramen, the end of the facial canal, is a curved aperture located on the temporal bone's inferior aspect of the petrous part, midway between the styloid process and the mastoid process. The facial nerve, which is the VII. cranial nerve, leaves the skull and the stylomastoid artery, that is a branch of the posterior auricular artery, enters the skull through the stylomastoid foramen (1-3).

The sensory and the motor roots of the facial nerve

Received: 19.04.2022 **Accepted:** 24.05.2022
Corresponding Author: Serdar Babacan, Harran University, Faculty of Medicine, Department of Anatomy, Sanlıurfa Turkey, **E-mail:** sbabacan@harran.edu.tr

arise from the sulcus bulbopontinus, on the anterior surface of the brain stem, between the pons and medulla oblongata. Both roots enter the internal auditory meatus in the temporal bone's petrosal part, accompanied by the vestibulocochlear nerve in the fossa cranii posterior. In the internal auditory meatus's lower part, the facial nerve gets into the facial canal and runs outward along with the inner ear. The facial nerve enlarges to form the geniculate ganglion and curves sharply posteriorly on the upper side of the promontorium when it reaches the inner wall of the tympanic cavity. It turns downward on the inner side of the entrance to the antrum mastoideum, on the posterior wall of the tympanic cavity, runs downward behind the pyramis, and leaves the temporal bone using the stylomastoid foramen, locates in front of the styloid foramen and the jugular foramen locates medially. After getting out from the stylomastoid foramen, 5-7 mm behind the mandibular ramus, the facial nerve gives off two branches; the digastric nerve and the posterior auricular nerve. After giving those branches the facial nerve, enters the parotid gland (4-7). The facial nerve's motor branches supply the mimetic and facial muscles (8).

The orbicularis oculi muscle around the eye is the sphincter muscle, innervated by the facial nerve. Facial nerve blockade is required to temporarily paralyze the orbicularis oculi muscle in order to prevent the increase in intraocular pressure that may occur due to squeezing of the eyelids during cataract extraction. Good anesthesia is important for safe intraocular surgery (9).

There have been four techniques described in the literature for facial nerve block: 1) Van Lint block, 2) Atkinson block, 3) O' Brien block, and 4) Nadbath block. According to Van Lint's block, the facial nerve's peripheral branches are blocked near the lateral orbital margin at the level of the external canthus of the eye, a point approximately 2 cm behind. In Atkinson's block, the upper branch of the facial nerve is blocked at the lower edge of the zygomatic bone. In O' Brien block, the main trunk of the facial nerve is blocked near the condylar process at the level of the mandibular neck. In Nadbath block, the facial nerve is blocked in the stylomastoid foramen. This technique is also called enhanced O' Brien block (9,10).

The blockage of the facial nerve trunk in the stylomastoid, Nadbath nerve block, is usually preferred because of the advantages in being less painful and preventing ecchymosis of the face, however, the risks of nerve injury and neurological severe complications may arise, also complications related to respiratory and vocal cords may develop as a result of inadvertent injection (11-13).

We aimed to develop linear regression formulas for determining the precise localization of the stylomastoid foramen on the base of the morphometric features of the person's own skull. Also to evaluate the distances between the surrounding anatomical structures, in addition to the mean and standard deviation values given in the literature, and to raise awareness for person-specific application instead of ambient values, on behalf of avoiding the complications.

MATERIAL AND METHOD

The study was conducted on 22 stylomastoid foramina (11 skulls) in the collection of Harran University Faculty of Medicine, Department of Anatomy. The dry skulls were photographed from inferior, lateral, anterior, and posterior plans in a standard position. Anthropometric points to be taken into account in measurements were determined (Figure 1). The 10 parameters determined for the stylomastoid foramen were measured on the photographs taken from the skull base (from inferior plane) (P1-10: Figure 2), and the 17 parameters determined for the morphometric features of the skull were measured on the photographs taken from the anterior plane (P11-18: Figure 3), lateral plane (P19-25: Figure 4), and posterior plan (P26,27: Figure 5) using Image J measurement software (Ver. 1.51 23 April 2018) (12).

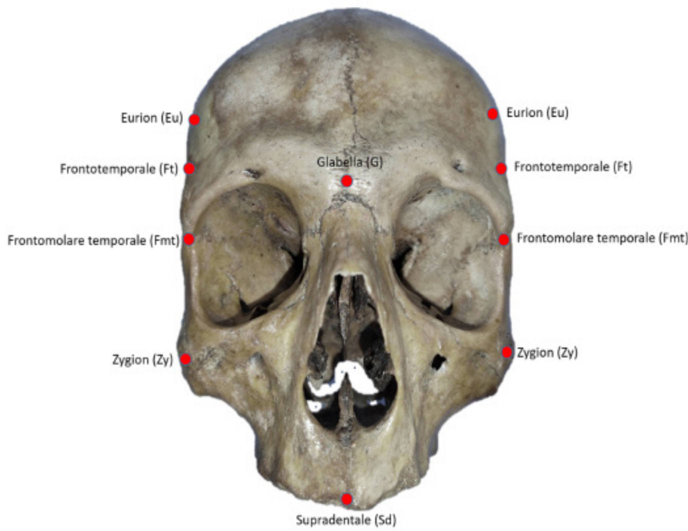

Figure 1. The anthropometric points used as landmark

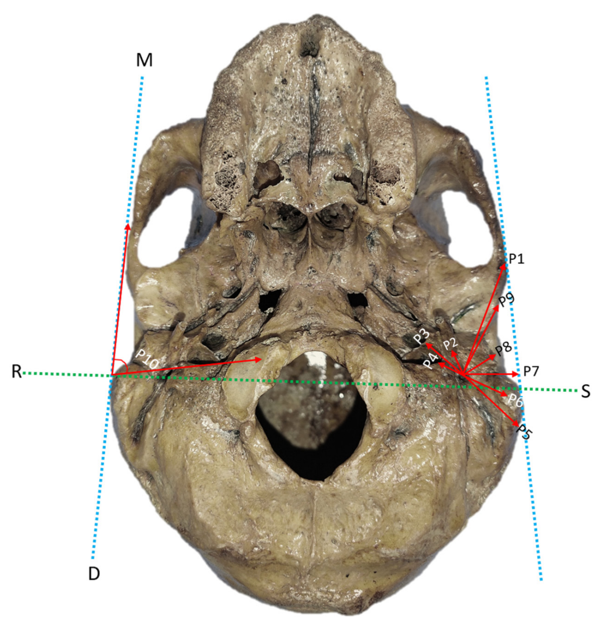

Figure 2. The parameters related to the stylomastoid foramen and surrounding anatomical structures (mm)

Table 1. The results of the descriptive statistics of the parameters related the stylomastoid foramen

Parameters (mm)	Min.	Max.	Mean ± SD
P1. The distance between the center of the stylomastoid foramen and the lateral margin of the root of the zygomatic arch	29.68	45.13	35.66±3.78
P2. The distance between the center of the stylomastoid foramen and the root of the styloid process	2.33	7.38	4.73±1.28
P3. The minimum distance between the center of stylomastoid foramen and the nearest carotid canal margin	5.80	19.53	13.91±2.81
P4. The minimum distance between the center of stylomastoid foramen and the nearest jugular foramen margin	2.95	9.47	6.57±1.69
P5. The distance between the posterior margin of the mastoid process and the center of the stylomastoid foramen	17.66	31.07	24.22±3.43
P6. The distance between the center of the stylomastoid foramen and the tip of the mastoid process	9.03	19.89	13.77±2.68
P7. The distance between stylomastoid foramen and MD line	13.74	21.38	17.54±2.33
P8. The distance between the center stylomastoid foramen and the inferior margin of the external acoustic meatus	6.66	15.08	10.55±1.92
P9. The distance between the center stylomastoid foramen and the lateral margin of the mandibular fossa	18.06	30.89	24.06±3.18
P10. MD-RS angle	54.16	85.99	66.54±9.49

Table 2. The descriptive statistics of the parameters related the skull dimensions

Parameters (mm)	Min.	Max.	Mean±SD
P11. The maximum skull breadth (Eu-Eu)	78.99	103.56	90.53±7.88
P12. The minimum distance between the two frontotemporale (Ft-Ft)	77.05	100.78	88.04±7.25
P13. The upper facial breadth (Fmt-Fmt)	79.94	101.56	92.56±7.25
P14. Orbital breadth	31.42	37.29	34.29±2.13
P15. Bizygomatic breadth (Zy-Zy)	81.37	104.31	93.14±6.88
P16. The orbital height	30.17	40.20	35.05±3.24
P17. The distance between Glabella (G) and supradentale (Sd)	71.57	101.12	84.31±9.43
P18. The distance between the lower margin of the maxilla and the orbit's lower margin	27.67	42.77	35.77±4.67
P19. The maximum antero-posterior breadth of the head (Op-G)	113.62	156.98	135.61±15.48
P20. The distance between the ophistocranion and the tip of the mastoid process	53.98	94.54	73.64±13.72
P21. The distance between the external margin of the external acoustic meatus the tip of the mastoid process	14.95	24.71	19.66±2.714
P22. The distance between the root of the zygomatic arch and the tip of the mastoid process	29.00	39.77	35.50±3.23
P23. The distance between the glabella and the tip of the mastoid process	84.23	106.24	101.59±2.83
P24. The distance between the zygoma ant the tip of the mastoid process	65.79	92.46	79.04±7.36
P25. The distance between the supradentale and the tip of the mastoid process	72.05	90.72	80.41±5.53
P26. The distance between parietal eminences	89.71	147.96	116.54±18.30
P27. The distance between bimastoid line and vertex	103.63	161.33	127.57±16.39

Table 3. The equations for estimating the distances between stylomastoid foramen and surrounding anatomical structures

Equations	Adjusted R^2	Standard Error of the Estimate
P1=18.758+(0.472xP12)-(2.092xP16)+(0.831xP17)–(0.390xP18)–(0.101xP20)	0.865	1.389
P2=-22.398+(0.302xP14)+(0.075xP17)+(0.048xP19)+(0.272xP21)+(0.110xP22)–(0.067xP24)	0.685	0.852
P3=-6.601+(0.497xP12)–(1.137xP16)+(0.368xP17)–(0.308xP18)–(0.087xP20)+(0.711xP21)–(0.309xP22)	0.382	2.206
P4=-24.927+(0.402xP12)–(0.456xP13)+(0.599xP14)+(0.574xP18)+(0.421xP22)	0.545	2.316
P5=22.783+(0.603xP12)–(0.649xP15)–(0.930xP16)+(0.313xP17)+(0.498xP18)–(0.704xP21)+(0.309xP22)	0.665	2.434
P6=9.639+(0.748xP11)–(0.876xP12)+(0.325xP18)–(0.274xP22)+(0.140xP24)	0.543	2.076
P7=79.566–(0.151xP11)–-(1.646xP14)+(0.662xP18)-(1.437xP21)+(0.010xP23)+(0.383xP24)–(0.243xP25)	0.387	1.828
P8=-12.657+(0.338xP15)–(0.071xP20)+(0.400xP21)+(0.452xP21)–(0.166xP25)	0.307	1.605
P9=-69.475+(0.697xP15)+(0.553xP16)–(0.442xP18)–(0.304xP20)+(1.384xP21)+(0.571xP22)	0.754	1.576
P10=-52.265–(3.819xP13)+(4.712xP15)+(0.886xP22)+(0.011xP23)	0.857	3.585

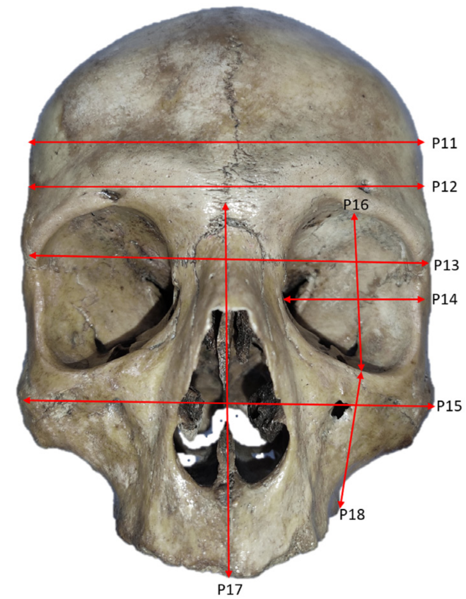

Figure 3. The parameters on the anterior aspect of the skull (mm)

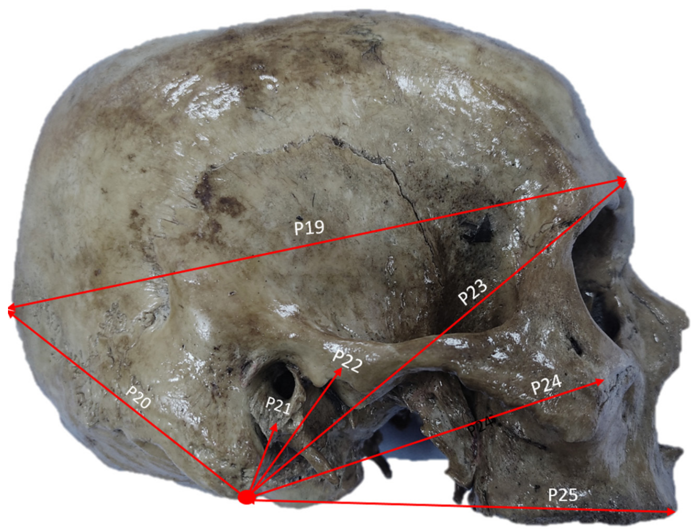

Figure 4. The parameters on the lateral aspect of the skull (mm)

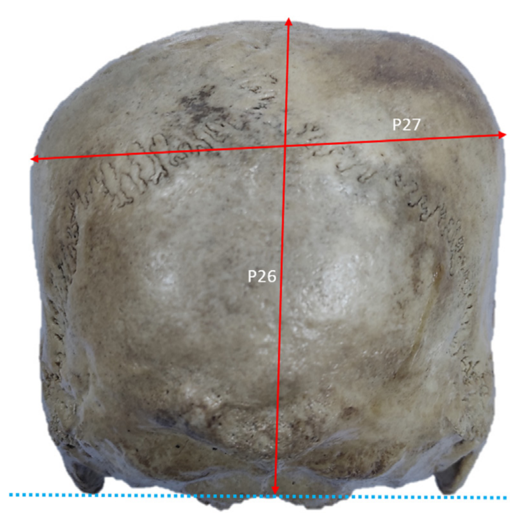

Figure 5. The parameters on the posterior aspect of the skull (mm)

Parameters

P1. The distance between the center of the stylomastoid foramen and the lateral margin of the root of the zygomatic arch

P2. The distance between the center of the stylomastoid foramen and the root of the styloid process

P3. The minimum distance between the center of stylomastoid foramen and the nearest carotid canal margin

P4. The minimum distance between the center of stylomastoid foramen and the nearest jugular foramen margin

P5. The distance between the posterior margin of the mastoid process and the center of the stylomastoid foramen

P6. The distance between the center of the stylomastoid foramen and the tip of the mastoid process

P7. The distance between the center stylomastoid foramen and the MD line (The line between the lateral margin of the zygomatic arch and the lateral margin of the mastoid process)

P8. The distance between the center stylomastoid foramen and the inferior margin of the external acoustic meatus

P9. The distance between the center stylomastoid foramen and the lateral margin of the mandibular fossa

P10. MD-RS angle (The angle between the MD line and RS line)

P11. The maximum skull breadth (Eu-Eu)

P12. The minimum distance between the two frontotemporale (Ft-Ft)

P13. The upper facial breadth (Fmt-Fmt)

P14. The orbital breadth

P15. The bizygomatic breadth (Zy-Zy)

P16. The orbital height

P17. The distance between the glabella (G) and the supradentale (Sd)

P18. The distance between the lower margin of the maxilla and the orbit's lower margin

P19. The maximum antero-posterior breadth of the head (Op-G)

P20. The distance between the ophistocranion and the tip of the mastoid process

P21. The distance between the external margin of the external acoustic meatus and the tip of the mastoid process

P22. The distance between the root of the zygomatic arch and the tip of the mastoid process

P23. The distance between the glabella and the tip of the mastoid process

P24. The distance between the zygoma and the tip of the mastoid process

P25. The distance between the supradentale and the tip of the mastoid process

P26. The distance between parietal eminences

P27. The distance between bimastoid line and vertex

Statistical analysis

As a result of the power analysis, when the effect size was selected as 0.5 (α=0.05) to examine the relationship between dependent variables and independent variables with the regression model, it was determined that approximately 22 (n=22) stylomastoid foramen should be included in the study for a significance level with power 0.80%. We performed statistical analyzes using IBM SPSS version 20.0 (IBM Corp. Released 2011. IBM SPSS Statistics for Windows, Version 20.0. Armonk, NY: IBM Corp.). The descriptive statistics values of the parameters related to the stylomastoid foramen and skull were evaluated. Pearson correlation analysis was applied to examine the relationship between the distances of the stylomastoid foramen to the surrounding anatomical structures and skull measurements. Equations to estimate the distances between the stylomastoid foramen and the surrounding anatomical structures were developed by linear regression analysis. The statistical significance level was $p<0.05$.

RESULTS

The results of the descriptive statistics values of the parameters related to the stylomastoid foramen were given in table 1.

The results of the descriptive statistics values of the parameters related to the skull dimensions were given in table 2.

The equations for estimating the distances between stylomastoid foramen and surrounding anatomical structures were given in table 3.

DISCUSSION

Blocking the facial nerve trunk in the stylomastoid foramen is a preferred method, but serious complications may occur due to incorrect injections and nerve injuries. Therefore, examining the morphometry of the stylomastoid foramen and the relationship with anatomical structures nearby is very important to avoid such dangers (9). Lindquist et al. reported that complications such as dysphonia, laryngospasm, unilateral vocal cord paralysis, and feeling of not being able to breathe develop as a result of blockade of the facial nerve trunk due to its proximity to the vagus, glossopharyngeal and accessory nerves (15).

The stylomastoid artery, which emerges from the stylomastoid foramen together with the facial nerve's trunk, masks the facial nerve, making the surgical approach difficult during parotidectomy (16).

The addition of epinephrine to local anesthetics or needle stimulation in the parapharyngeal region may trigger the vascular sympathetic response. As a result, facial nerve palsy may occur due to ischemia of the stylomastoid foramen (17).

Anatomical knowledge of the stylomastoid foramen is important for clinical applications because of its proximity to important neurovascular structures. Any anatomical variation may present with compression symptoms. In addition, the surgical anatomy of the stylomastoid foramen is important (3).

The identified landmarks for the facial nerve trunk should be easy to identify and reliable. Because of their hard and reliable anatomical location, although difficult to palpate the bony structures are more suitable than soft tissue or cartilaginous landmarks (18).

Sharma and Varshney (2015) studied on 100 dry skulls in 2015. They found that 83.51% of the stylomastoid foramen was located anterior to the XY line (The horizontal line passing through the tip of the anterior edge of both mastoid processes), 13.4% along the XY line 3.03% posterior to the XY line (9).

Kutoğlu et al. (2021) studied on 53 temporal bones in 2021 and they found 54.7% of the stylomastoid foramen was located anterior to the XY line, 34% posterior to the XY line, and 13.3% above the XY line (19).

Sharma and Varshney (2015) evaluated the distance between the tip of the mastoid process center and the center of the stylomastoid foramen; and as 15.26±1.4mm on the right side and 14.32±1.8mm on the left side. They found the distance between the jugular foramen and the center of the stylomastoid foramen as 12.28±1.9mm and 12.96±2.1mm (respectively on the right side and left side). They found the angle as 66.57±2.6 and 65.96±1.8 on the right and left sides, respectively, in degree (9).

Jai Rexlin et al., (2019) studied on 40dry human skulls in 2019. They found the distance between the center of the stylomastoid foramen to the center of the jugular foramen as 8.90±1.42mm and 9.34±1.46mm (on the left and right sides respectively). They measured the shortest distance between the mastoid process and the center of the stylomastoid foramen as 13.42±1.97mm on the left side and 13.77±1.64mm on the right side (4).

In the current study, we found the distance between the root of the styloid process and stylomastoid foramen as 4.73±1.28mm, the distance between the jugular foramen and the stylomastoid foramen was 6.57±1.69mm, the distance between the mastoid process and the stylomastoid foramen was 13.77±2.68mm, MD-RS angle was 66.54±9.49 in degree.

CONCLUSION

The size of the range between the minimum and maximum values in the tables (table 1 and table 2) as a result of the descriptive statistics and the different measurements in between with other studies reveal that the results may vary among the people and also populations. For this reason, mean values can give misleading information in determining the topographical relationship between the stylomastoid foramen and the surrounding anatomical structures. We have developed regression formulas that will estimate the accurate location of the stylomastoid foramen and the precise distances between other surrounding anatomical structures, taking into account the morphometric characteristics of the person's own skull. It is noteworthy that the power of the equations produced for P1 and P10 among the developed formulas is high. We think that the power of the equations related to other parameters will increase with the increase in sample size. We believe that this new technique we have developed will guide anesthesiologists and surgeons in person-specific approaches.

Acknowledgements: *The authors sincerely thank those who donated their bodies to science so that anatomical research can be done. That's why these donors and their families deserve our deepest gratitude.*

Financial disclosures: *The authors declared that this study hasn't received no financial support.*

Conflict of Interest: *The authors declare that they have no competing interest.*

Ethical approval: *The authors declare that the current study on donated cadaver skulls belonging to the Department of Anatomy was carried out in accordance with the 1964 Declaration of Helsinki. There were no human participants in the study or there was no human/animal experimentation, therefore no ethics committee approval.*

REFERENCES

1. Ghosh SK, Narayan RK. Variations in the morphology of stylomastoid foramen: a possible solution to the conundrum of unexplained cases of Bell's palsy. Folia Morphol. 2021;80:97-105.
2. Ho ML, Juliano A, Eisenberg RL, Moonis G. Anatomy and pathology of the facial nerve. Am J Roentgenol. 2015;204: 612–9.
3. Swetaa A, Mohanraj KG, Morphometric study of petrosquamous part of the temporal bone with reference to stylomastoid foramen. Drug Invention Today. 2019;12:2137-9.
4. Jai Rexlin PE, Sangeetha S, Premavathy D. Morphometry of stylomastoid foramen and its clinical applications. Drug Invention Today. 2019;11:2593-6.
5. Seneviratne SO, Patel BC. Facial Nerve Anatomy and Clinical Applications. [Updated 2021 Jul 31]. In: StatPearls [Internet]. Treasure Island (FL): StatPearls Publishing; 2022 Jan-. Available from: https://www.ncbi.nlm.nih.gov/books/NBK554569/
6. Takezawa K, Townsend G, Ghabriel M. The facial nerve: anatomy and associated disorders for oral health professionals. Odonthology. 2018;106:103-16.
7. Warwick R, Williams PL. Gray's anatomy. 35th ed. Edinburgh: Longman Group Ltd. 1973
8. Pascual P, Moralinno E, Vasquez T, et al. Extracranial course of the facialnerve revisited. Anatomical Record. 2019;302:599-608.
9. Sharma N, Varshney R. Morphometry of stylomastoid foramen and its clinical application in facial nerve block. Saudi J Anesthesia. 2015;9;60-3.
10. Schimek F, Fahle M. Techniques of facial nerve block. Br J Ophthalmol. 2015;79:166-173.
11. Warner LO, Martino JD, Davidson PJ. Pulmonary edema after Nadbath and retrobulbar blocks: A possible explanation. Anesth Analg. 1995;80:643.
12. Birt CM, Dixon WS, Dionne CL. Vocal cord paralysis with Nadbath facial block. Can J Ophthalmol. 1994;29:231-3.
13. Zahl K. Selection of techniques for regional blockade of the eye and adnexa. In: McGoldrick KE, ed. Anesthesia for Ophthalmic and Otolaryngologic Surgery. Philadelphia, PA: WB Saunders Co. 1992:235-47.
14. Schneider CA, Rasband WS, Eliceiri KW. NIH Image to ImageJ: 25 years of image analysis. Nature Methods. 2012;9:671-5.
15. Lindquist TD, Kopietz LA, Spigelman AV, et al. Complications of Nadbath facial nerve block and a review of the literature. Ophthalmic Surg. 1988;19:271-3.
16. Moreu S, Bourdon N, Salame E, et al. Facial Nerve: Vascular Related Anatomy at The Stylomastoıd Foramen. Ann Owl Rhinol Lury. 2000;109:849-52.
17. Lubszczyk M, Luczynska-Sopel A, Polaczkiewicz D. Facial nerve palsy and laryngospasm as a complication of local anaesthesia during adenotonsillectomy. Auris Nasus Larynx. 2018;45:1113-5.
18. Greyling LM, Glanvill R, Boon JM, et al. Bony landmarks as an aid for intraoperative facial nerve identification. Clin Anat. 2007;20:739-44.
19. Kutoğlu T, Çetkin M, Turan Ö, et al. Morphometric and Topographic Features of Stylomastoid Foramen and its Clinical Significance in Facial Nerve Block. J Neurol Surg B Skull Base. 2021;82:e271-7.